

RESEARCH

Open Access



Intestinal microflora and metabolites affect the progression of acute pancreatitis (AP)

Zhenjiang Wang^{1†}, Mingyi Guo^{1†}, Sen Yang¹, Yuping Chen¹, Jianbin Cheng¹, Zaiwei Huang¹, Tongxu Wang¹, Xiaobei Luo², Xingxiang He³, Dali Wang^{1*} and Xiaohong Xu^{1*}

Abstract

Specific intestinal metabolites are closely associated with the classification, severity, and necrosis of acute pancreatitis (AP) and provide novel insights for in-depth clinical investigations. In this study, the gut microbiota and metabolites of 49 AP patients at different treatment stages and severities were analysed via 16S rDNA sequencing and untargeted metabolomics to investigate the trends in gut microbiota composition and metabolome profiles observed in patients with severe AP. These findings revealed an imbalance in intestinal flora homeostasis among AP patients characterized by a decrease in probiotics and an increase in opportunistic pathogens, which leads to damage to the intestinal mucosal barrier through reduced short-chain fatty acid (SCFA) secretion and disruption of the intestinal epithelium. This dysbiosis influences energy metabolism, anti-inflammatory responses, and immune regulation, and these results highlight significant differences in energy metabolism pathways. These findings suggest that the differential composition of intestinal flora, along with alterations in intestinal metabolites and metabolic pathways, contribute to the compromised integrity of the intestinal mucosal barrier and disturbances in energy metabolism in patients with severe AP.

Keywords Acute pancreatitis, Gastrointestinal microbiota, Metabolite/metabolic pathways, Severe trend, Multiple omics

Introduction

Acute pancreatitis (AP) is a prevalent gastrointestinal emergency that is characterized by the premature activation of pancreatic enzymes, which results in local pancreatic inflammation and potentially systemic inflammatory response syndrome [1]. The course of acute pancreatitis varies and is often challenging to predict during its early

stages. Approximately 80% of patients experience mild to moderate AP without organ failure and this lasts more than 48 h [2], whereas the remaining 20% progress to severe acute pancreatitis (SAP). Overall, the mortality rate can reach 30% [3]. There has been extensive research focused on understanding the pathogenesis, treatment, and outcome of AP. Early recognition and prevention of severe AP are crucial challenges in the medical field. In recent years, increasing attention has focused on studying the gut microbiota and metabolic disorders in AP patients. With advancements in metabolomics technology and deeper investigations into AP, numerous studies have identified specific metabolites in both the gut and serum that are closely associated with the classification, severity, pancreatic inflammation, and necrosis of AP [4–8]. Previous studies have primarily focused on cross-sectional metabolomics analyses among AP patients;

[†]Zhenjiang Wang and Mingyi Guo have contributed equally to this work.

*Correspondence:

Dali Wang
wangdali770712@163.com

Xiaohong Xu
xuxiaohong0451@sina.com

¹ Zhuhai People's Hospital (Zhuhai Clinical Medical College of Jinan University), Zhuhai, China

² Nanfang Hospital, Southern Medical University, Guangzhou, China

³ The First Affiliated Hospital of Jinan University, Guangzhou, China



however, the gut microbiota plays a significant role as an important disease-related factor closely linked to the occurrence, progression, and severity of AP [9–13]. Currently, few studies have investigated the associations between gut metabolites and microbial diversity in patients with AP, and longitudinal studies encompassing different stages of the disease are lacking. In this study, we conducted a comprehensive analysis via 16S rDNA sequencing combined with untargeted metabolomics to explore differential flora, metabolites, and metabolic pathways at various stages and severity levels of AP. Our findings provide crucial theoretical foundations and insights for guiding personalized treatment approaches for AP patients as well as strategies for preventing and managing severe cases through targeted faecal microbiota transplantation.

Study subjects and groups

This study was approved by the Ethics Committee of Zhuhai Hospital Affiliated with Jinan University (Zhuhai People’s Hospital) and the approval number was (2022) Ethical Review [research] NO. (40). All patients provided written informed consent. We conducted the experiments according to the official guidelines issued by the National Health and Family Planning Commission.

In this study, we included 49 patients with a definite diagnosis of AP. Patients were divided into mild acute pancreatitis (MAP, n=32) and severe acute pancreatitis

(SAP, n=17) groups according to disease severity. Groups were divided according to disease stage and the acute phase (A) and recovery phase (R) (Fig. 1). The severity of AP was diagnosed according to the Chinese Guidelines for the Diagnosis and Treatment of Acute Pancreatitis [15].

Materials and methods

Data collection

Stool samples were collected from acute pancreatitis (AP) patients at two time points: within 72 h of symptom onset and 1 month after hospital discharge. To prevent contamination, patients were instructed to empty their bladder before providing the stool sample. A sterile collection box or other sterile collector was positioned at the rear of the toilet to ensure that the stool was discharged directly into the container. Researchers either washed their hands thoroughly or wore sterile gloves while handling the samples. The cover of a 2 mL sterile freezer tube was unscrewed, and the sampling spoon provided was used to collect a portion of the stool sample. The surface layer of the stool was discarded, and a sample from within the stool was collected instead. Approximately 50 mg of stool, about the size of one to two mung beans, was transferred into the freezer tube using the spoon. The tube was then tightly sealed, placed in a self-sealing bag, and securely sealed. Immediately after collection, the stool samples were snap-frozen in liquid nitrogen and

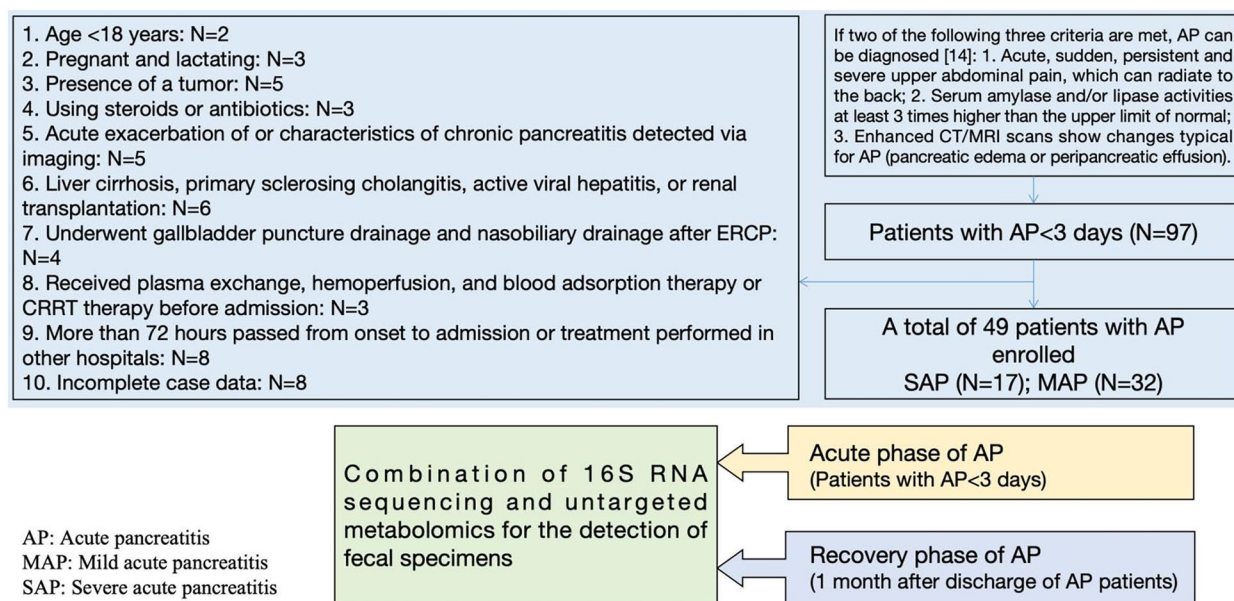


Fig. 1 Research design flowchart

stored at -80°C until further processing for 16S rDNA sequencing and untargeted metabolome analysis.

16S rDNA method

DNA extraction and sequencing

Total faecal microbial DNA was obtained with a Faecal Genome DNA Extraction Kit (AU46111-96, BioTeke, China) according to the manufacturer's instruction manual. DNA was quantified with a Qubit instrument (Invitrogen, USA). Total DNA was amplified via PCR using the universal primers 341F/805R (V3-V4, 341F: 5'-CCTACGGGNGGCWGCAG-3'; 805R: 5'-GAC TACHVGGGTATCTAATCC-3'). Phusion® Hot Start Flex 2X Master Mix was the enzyme used for PCR. PCR amplification conditions were as follows: predenaturation at 98°C for 30 s; 32 cycles of denaturation at 98°C for 10 s, annealing at 54°C for 30 s, extension at 72°C for 45 s; and a final extension at 72°C for 10 min. The PCR product was purified via AMPure XT Beads (Beckman Coulter Genomics, Danvers, MA, USA) and quantified via Qubit (Invitrogen, USA). Qualified PCR products were evaluated via an Agilent 2100 Bioanalyzer (Agilent, USA) and Illumina library quantitation kits (Kapa Biosciences, Woburn, MA, USA); products were then pooled and sequenced via a NovaSeq 6000 SP (NovaSeq 6000 SP Reagent Kit v1.5), the libraries were sequenced via the NovaSeq PE250 platform, which was provided by LC-Bio Technology Co., Ltd., Hangzhou, China.

Data processing and 16S rDNA sequencing analysis

The data processing steps began with the removal of sequencing primers from the demultiplexed raw sequences using Cutadapt (v1.9). After this initial cleaning, paired-end reads were merged with FLASH (v1.2.8)¹⁶, which efficiently combines overlapping sequences to enhance data integrity. Low-quality reads were then filtered out using fqtrim (v0.94), where sequences with quality scores below 20, those shorter than 100 base pairs, and reads containing more than 5% "N" records were trimmed. This step was crucial for ensuring that only high-quality clean tags were retained for further analysis. Chimeric sequences were subsequently filtered using Vsearch software (v2.3.4) to eliminate any erroneous sequences that could impact the results.

Following quality control, DADA2¹⁷ was utilized for denoising and generating amplicon sequence variants (ASVs), providing a more accurate representation of the microbial community. For taxonomic classification, sequence alignment was performed using the QIIME2 plugin feature classifier, referencing the SILVA (Release 138) and NT-16S databases to enhance the accuracy

of species annotation. Alpha and beta diversities were calculated using QIIME2¹⁸, and relative abundance data was analyzed to understand the composition of bacterial communities. We employed PERMANOVA (permutational multivariate analysis of variance) for the beta-diversity analysis. The Wilcoxon test was applied to identify differentially abundant genera, with a significance threshold of $p < 0.05$. Finally, visual representations of the data were created using R packages, such as Vegan and ggplot2, to effectively communicate the findings related to the impact of intestinal flora and metabolites on the progression of acute pancreatitis.

Metabolite extraction and liquid chromatography–mass spectrometry (LC–MS) analysis

Metabolite extraction

The collected samples were thawed on ice, and metabolites were extracted from 20 μL of each sample via the addition of 120 μL of precooled 50% methanol buffer. The mixture of metabolites was subsequently vortexed for 1 min, incubated for 10 min at room temperature, and stored at -20°C overnight. The mixture was centrifuged at $4000\times g$ for 20 min, and the supernatant was transferred to 96-well plates. Samples were stored at -80°C prior to LC–MS analysis. Pooled quality control (QC) samples were also prepared by combining 10 μL of each extraction mixture.

LC–MS analysis

All samples were analysed via a TripleTOF 5600 Plus high-resolution tandem mass spectrometer (SCIEX, Warrington, UK) in both positive and negative ion modes. Chromatographic separation was performed via an ultra-performance liquid chromatography (UPLC) system (SCIEX, UK). An ACQUITY UPLC T3 column (100 mm \times 2.1 mm, 1.8 μm , Waters, UK) was used for reversed-phase separation. For the separation of metabolites, the mobile phase consisted of solvent A (water, 0.1% formic acid) and solvent B (acetonitrile, 0.1% formic acid). Gradient elution was performed at a flow rate of 0.4 mL/min as follows: 5% solvent B for 0–0.5 min; 5–100% solvent B for 0.5–7 min; 100% solvent B for 7–8 min; 100–5% solvent B for 8–8.1 min; and 5% solvent B for 8.1–10 min. The column temperature was maintained at 35°C . The TripleTOF 5600 Plus system [19] was used to detect metabolites eluted from the column. The curtain gas pressure was set at 30 PSI, and the ion source gas 1 and 2 pressures were set at 60 PSI. The interface heater temperature was 650°C . In positive-ion mode, the ion spray floating voltage was set at 5 kV and in negative-ion mode it was set at -4.5 kV. The MS data were acquired in information-dependent acquisition (IDA) mode. The TOF mass range was 60–1200 Da.

Survey scans were acquired every 150 ms, and as many as 12 product ion scans were collected if the threshold of 100 counts/s was exceeded with a 1+ charge state. The total cycle time was fixed at 0.56 s. Four-time bins were summed for each scan at a pulse frequency of 11 kHz by monitoring the 40 GHz multichannel Time-to-Digital Converter (TDC) detector with four-anode/channel detection. The dynamic exclusion was set for 4 s. During the entire acquisition period, the mass accuracy was calibrated every 20 samples. Furthermore, a QC sample was analysed every 10 samples to evaluate the stability of the LC–MS [20].

Metabolomics data processing

The acquired LC–MS data were pretreated via XCMS software [21] (<http://metlin.scripps.edu/download/>). The raw data files were converted into mzXML format and then processed via the XCMS, CAMERA [22] and metaX [23] toolbox in R. Each ion was identified by comprehensive information on the retention time and m/z. The intensity of each peak was recorded, and three-dimensional matrix containing arbitrarily assigned peak indices (retention time–m/z pairs), sample names (observations) and ion intensity information (variables) were generated. The information was subsequently matched to in-house (LC-Bio Technology Co., Ltd., Hangzhou, China) and public databases. The open access Kyoto Encyclopedia of Genes and Genomes (KEGG, <https://www.genome.jp/kegg/pathway.html>) and the Human Metabolome Database (HMDB, hmdb.ca/metabolites) databases were used

to annotate the metabolites by matching the exact molecular mass data (m/z) to those from the database within a threshold of 10 ppm. The peak intensity data were further preprocessed via metaX. Features that were detected in <50% of the QC samples or 80% of the test samples were removed, and values for missing peaks were extrapolated with the k-nearest neighbour algorithm to further improve the data quality. PCA was performed to detect outliers and batch effects via the preprocessed dataset. QC-based robust locally weighted scatterplot smoothing (LOESS) signal correction (QCRLSC) was fitted to the QC data according to the order of injection to minimize signal intensity drift over time. In addition, the relative standard deviations of the metabolic features were calculated across all QC samples and those with standard deviations >30% were removed. The group datasets were normalized before the analysis was performed. Data normalization was performed on all samples via the probabilistic quotient normalization algorithm. Then, a QC-robust spline batch correction was performed on the QC samples. Differentially abundant metabolites were selected according to the P value determined by Student's t-test and adjusted for multiple tests via an FDR (Benjamini–Hochberg). We also conducted supervised partial least squares discriminant analysis (PLS-DA) using metaX for variables detected by the discriminant profiling statistical method to identify more specific differences between groups. A variable importance in projection (VIP) cut-off value of 1.0 was set to select important features.

Software parameters

XCMS		metaX		MS2 identification	
Item	Parameter	Item	Parameter	Item	Parameter
Method	centWave	Adduction	pos: [M+H] ⁺ , [M+Na] ⁺ , [M+K] ⁺ , [M+NH ₄] ⁺ neg: [M-H] ⁻ , [M+NH ₄ -2H] ⁻ , [M+2C] ²⁻ , [2 M-3H] ³⁻	MS1 mass tolerance	0.01 Da
minfrac	0.5			MS2 mass tolerance	0.05 Da
snthr	6	MS1 mass tolerance	10 ppm	Identification score cut off	75%
ppm	30	Database	KEGG, HMDB	Database	In-house, Massbank, HMDB, Lipidblast
peakwidth	5, 25				
bw2	5				
mzwid	0.015				
mzdiff	0.01				
profStep.OBIWarp	0.1				

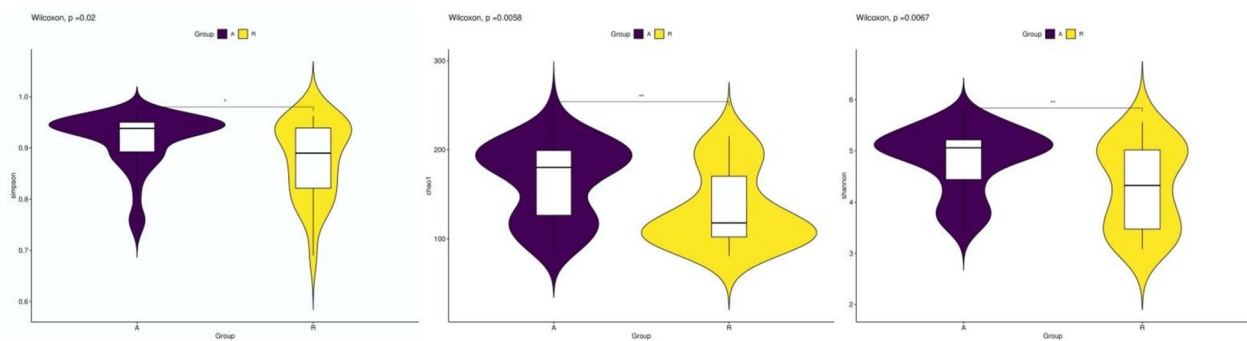


Fig. 2 Alpha diversity violin plots (Simpson, Chao1 and Shannon indices) showing significant differences in alpha diversity between acute and recovery phases (A vs. R) in AP patients

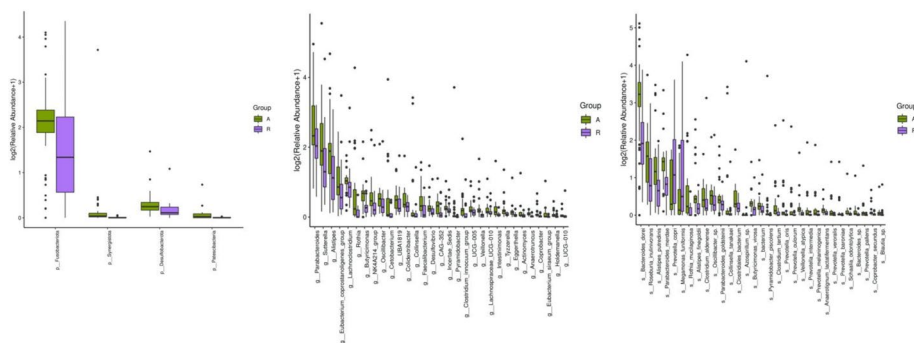


Fig. 3 Mann–Whitney U test was used to showed the differential abundance of taxa in Groups A and R (phylum, genus, and species levels). The horizontal axis of the chart represents the distinct species, which are arranged from left to right according to their abundance, whereas the vertical axis indicates their relative abundance. Heights of the columns provide a visual means to assess the abundance of each distinct species within different groups

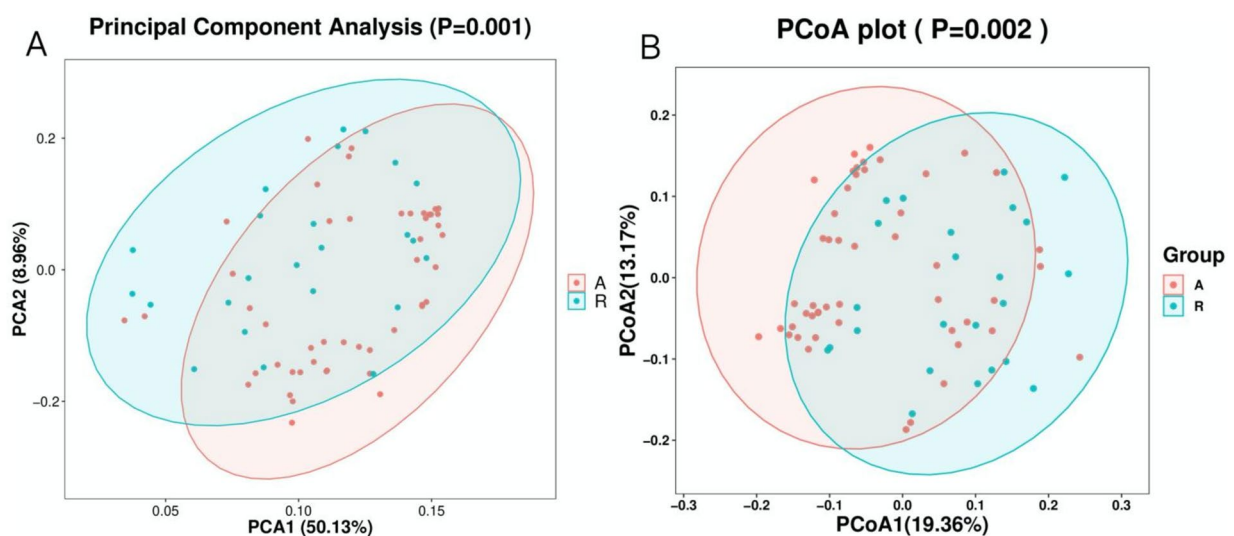


Fig. 4 **A** PCA. Principal Component Analysis (PCA) revealed significant differences in species diversity of AP patients with different disease stages (A vs. R), ($p=0.001$, PERMANOVA). **B** PCoA (unweight_unifrac_pcoa). Principal coordinate analysis (PCoA) revealed differences in sample species diversity among AP patients with different disease stages (A vs. R), ($p=0.002$, PERMANOVA)

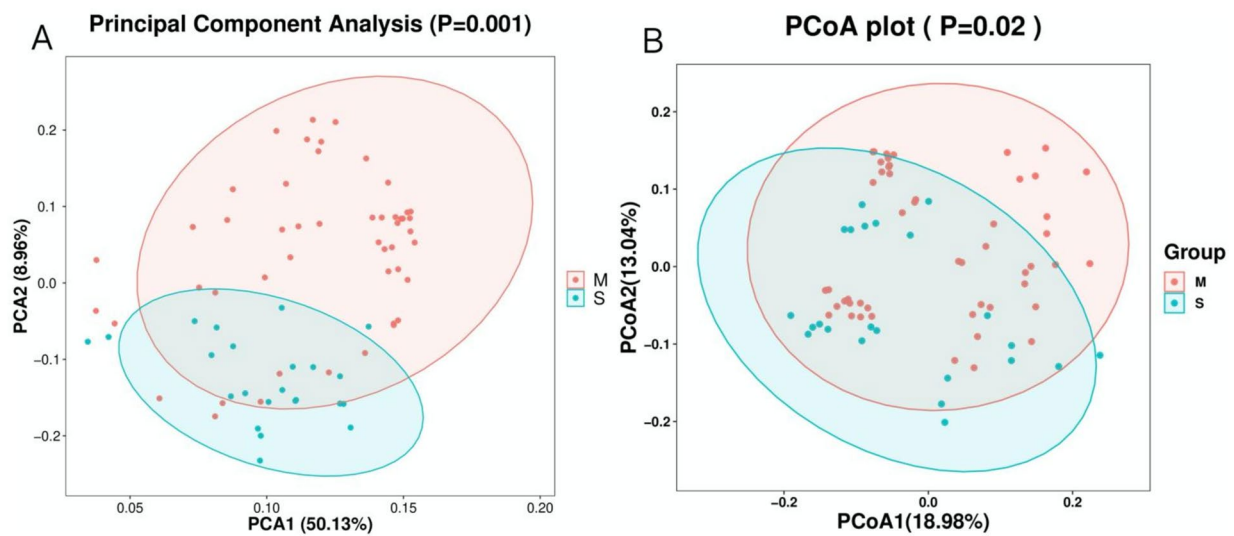


Fig. 7 **A** PCA. Principal Component Analysis (PCA) revealed significant differences in species diversity of AP patients with different disease stages (M vs. S), ($p=0.001$, PERMANOVA). **B** PCoA (unweight_unifrac_pcoa). Principal coordinate analysis (PCoA) revealed differences in sample species diversity among AP patients with different disease stages (M vs. S), ($p=0.02$, PERMANOVA)

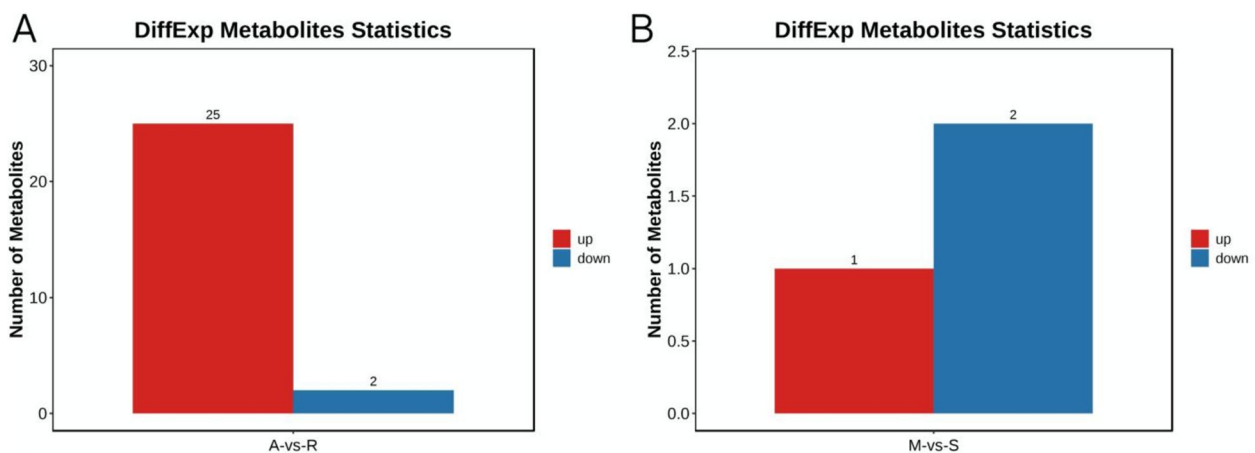


Fig. 8 Differentially abundant metabolite profiles were observed between the disease and recovery phases (**A**) and between mild and severe cases (**B**) in patients with AP

Variations in intestinal metabolites among patients at different stages of treatment and severity of acute pancreatitis

The metabolite profiles of patients with AP were significantly different between the active and recovery stages of the disease as were those of patients in different severity groups. Figure 8 illustrates the discernible metabolic disparities observed between the two groups, and the specific metabolites are detailed in Tables 1 and 2.

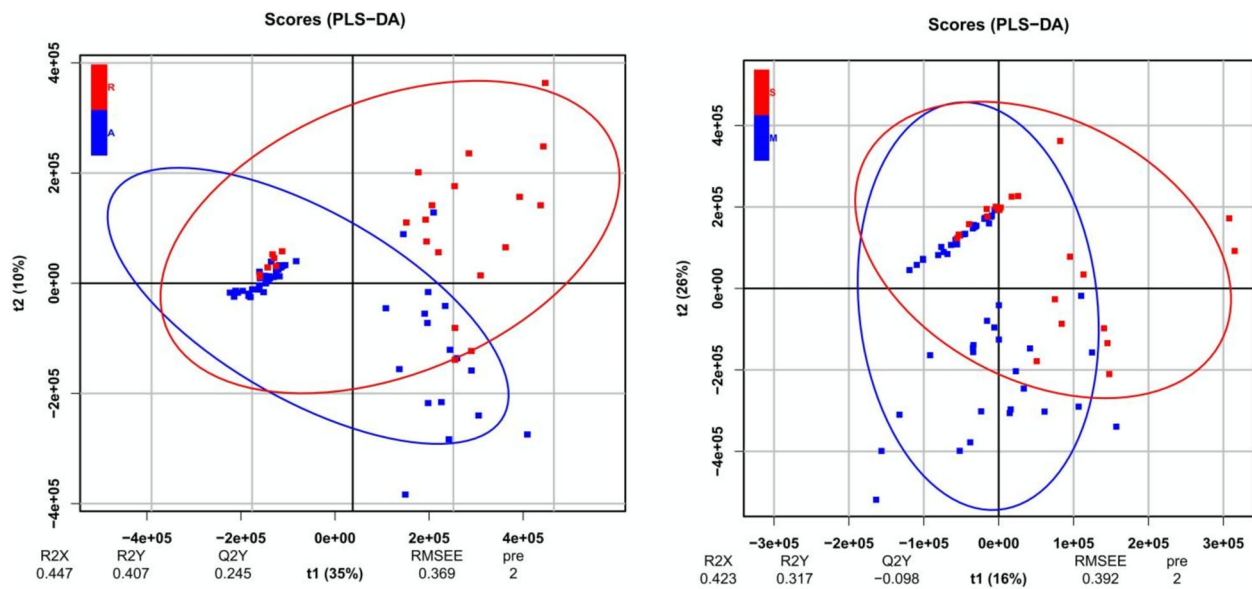
The reliability of metabolic differences between groups was assessed via partial least squares discriminant analysis (PLS-DA), and separate PLS-DA models were constructed for pairwise group comparisons. Higher values of the model parameters R^2 and Q^2 indicated greater reliability of the current PLS-DA model. Permutation tests were conducted on R^2 and Q^2 to validate the model's performance. Figure 9 illustrates the PLS-DA between the mild and severe groups, whereas Fig. 10 displays the permutation plot.

Table 1 Significantly and differentially abundant metabolites in A vs. R (partial)

Index	A_mean	R_mean	log2_FC	P value	FDR	VIP	Metabolites
C04483	718336084.4	4193134868	2.54529834	1.16E-06	0.000304268	8.099668831	Deoxycholic acid
C00423	6626302717	3077223910	-1.10657469	0.028877043	0.17066657	6.804105236	trans-Cinnamic acid
C00695	1274731590	3577132667	1.488610123	0.011281393	0.118875447	5.337333633	Cholic acid
C02528	360053252.8	1640154055	2.187549123	2.52E-05	0.002654955	5.254528248	Chenodeoxycholic Acid
C00431	792393338.8	2164169483	1.449524828	0.025873602	0.1680187	4.009617488	5-Aminovaleric acid
C09126	56476560.9	901771235.1	3.997037347	0.0021639	0.054200534	3.80315974	Genistein
C06563	88943559.25	912136348.6	3.358287455	0.002759813	0.055216829	3.750516401	Genistein
C00137	81497749.02	881837647.7	3.435680953	0.01397791	0.125470021	3.588951795	Inositol
C01477	88025732.5	628785951.5	2.836571752	0.042595327	0.21018584	3.004376647	Apigenin
C00318	83051734.78	621389066.4	2.903414648	0.008101636	0.10005094	2.660017245	L-Carnitine

Table 2 Significantly and differentially abundant metabolites in M vs. S

Index	M_mean	S_mean	log2_FC	P value	FDR	VIP	Metabolites
C07056	1305175288	528867159.5	-1.303266279	0.049940997	0.815689187	4.226556086	Isoproterenol
C17726	493041472.7	169490502.4	-1.540504573	0.011556045	0.815689187	3.158033254	Muricholic acid
C00417	3306408.508	41041984.61	3.633763609	0.036751543	0.815689187	1.022580801	cis-Aconitic acid

**Fig. 9** PLS-DA (A and R, M and S). A PLS-DA score plot of AP patients with different disease stages (A vs. R) and different severities (M vs. S) is shown based on LC-MS technology. Ellipses of different colors in the PLS-DA model distribution plot represent 95% confidence intervals.

Differences in metabolic pathways in patients with different treatment stages and severities of AP

Through functional annotation and enrichment of metabolites, we obtained pathways affected by the differentially abundant metabolites. Figure 11 shows the KEGG functional enrichment results for differentially

abundant metabolites in the acute and recovery phases of AP (Fig. 11A) and in mild and severe cases (Fig. 11B). For differentially abundant metabolites between disease stages, the primary bile acid biosynthesis pathway emerged as the most significant pathway and plays a pivotal role in bile acid synthesis. For

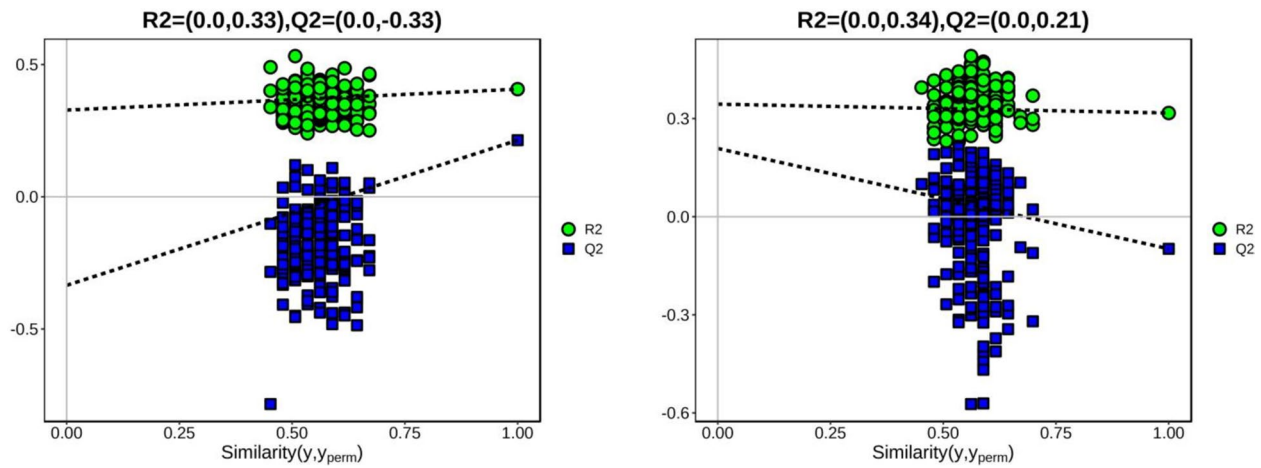


Fig. 10 Permutation (A and R, M and S). A permutation plot comparing disease stages (A vs. R) and severities (M vs. S) among acute pancreatitis (AP) patients. The permutation test chart corresponds to the Partial Least Squares Discriminant Analysis (PLSDA) model, which evaluates overfitting. Data were generated through 200 rounds of 70% cross-validation of the PLSDA model, with no specific data points displayed

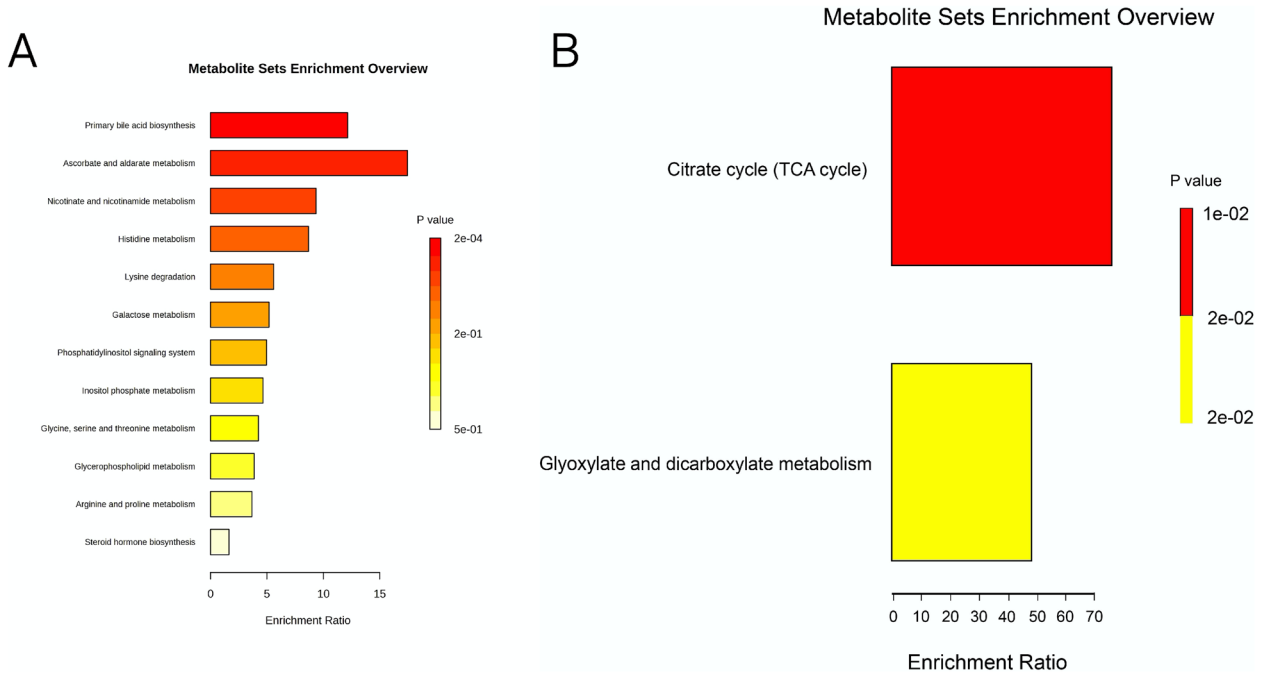


Fig. 11 By annotating and enriching the functions of metabolites, we identified pathways influenced by differentially abundant metabolites. **A** Enriched pathways in the A and R stages of AP. **B** Enriched pathways in the mild and severe stages of AP

the differentially abundant metabolites between mild and severe symptoms, we identified alterations in the TCA cycle pathway and the glyoxylate and dicarboxylate metabolism pathways. The TCA cycle represents a fundamental route for intracellular energy production,

whereas the glyoxylate and dicarboxylate metabolism pathways are involved in carbon metabolism and organic acid metabolism within cells and thereby maintain the metabolic balance within organisms.

Discussion

Increasing evidence demonstrates that the composition of the intestinal microbiome differs between healthy and diseased states and that an imbalanced microbiome can contribute to alterations in the pathophysiology of gastrointestinal diseases and extraintestinal conditions such as pancreatitis [24]. Furthermore, metabolites derived from the gut microbiota play crucial roles in the progression of AP with some exerting beneficial effects and others exerting harmful effects. Host-beneficial metabolites include lactic acid, secondary bile acids (BAs), short-chain fatty acids (SCFAs), and bacteriocins, which are generally acknowledged as antimicrobial factors. They play pivotal roles in preventing pathogen infections and regulating immune responses [25, 26]. This study investigated the role of intestinal microbiota and metabolites in the progression of AP by analysing changes in their composition and metabolic pathways at different stages and severity levels. Understanding the importance of the intestinal microbiota and metabolites in the progression of AP and the possible progression mechanisms of AP to severe cases has important clinical implications for the early prediction of disease progression and may reveal the possible mechanisms of this progression.

Imbalanced gut microbiota in SAP patients worsens disease severity by affecting the intestinal barrier, energy metabolism, and immune response

Differences in the microbiota at different disease stages

At the phylum level, abundances of specific microorganisms, such as *Synergistota*, *Patescibacteria*, *Desulfobacterota* and *Fusobacteriota*, were significantly greater in patients with active AP than in those in recovery. *Synergistota* has been shown to be associated with inflammatory responses [27]. The abundance of *Desulfobacterota* was increased in patients with active AP, which is usually associated with the sulphate reduction reaction and changes in its abundance may cause an inflammatory response, affect intestinal epithelial cells, and damage the intestinal mucosal barrier. Huang et al. [28] reported that *Desulfobacterota* may release lipopolysaccharide (LPS) into the intestine and cause an inflammatory response, and *Desulfobacterota* also disrupts intestinal energy metabolism. *Fusobacteriota* have been studied in other diseases and are associated with chronic inflammation and tumour development [29]. In the context of AP, the dominant microbiota associated with intestinal inflammation exacerbates the inflammatory response and disrupts intestinal immune homeostasis and thereby impacts the host's disease condition. From an intestinal

microecological perspective, the recovery from AP is accompanied by the restoration of both the composition and function of the intestinal flora.

Significant differences in the gut microbiota among patients with different severities of AP

The intestinal microecology and its functionality serve as crucial indicators for assessing AP severity. For example, *Verrucomicrobiota* was significantly lower in patients with severe AP than in those with mild AP. *Verrucomicrobiota* is predominantly found in the inner layer of the intestinal mucosa and can degrade polysaccharides, such as mucosaccharides and cellulose, and thereby provides energy and nutrients. Additionally, *Verrucomicrobiota* can synthesize SCFAs, including propionic acid and butyric acid, which have been shown to increase the expression of the intestinal mucin MUC2 by inducing MUC2 mRNA expression in the human goblet cell line LS174T [30] and consequently improving intestinal mucosal barrier function. Increased mucin production and MUC2 gene expression have been shown to be influenced by short-chain fatty acids (SCFAs), particularly butyrate, which is produced through the fermentation of dietary fibers by gut microbiota. Several studies have demonstrated that SCFAs play a crucial role in regulating MUC2 expression by enhancing the stability of MUC2 mRNA, leading to elevated levels of MUC2 protein in intestinal epithelial cells. This regulation is vital for maintaining the integrity of the intestinal mucosal barrier, which protects against pathogens and contributes to overall gut health. *Akkermansia muciniphila* (AKK) was the first discovered member of *Verrucomicrobiota*. AKK bacteria enhance immunity by improving the host's intestinal barrier and gut microbiota stability and improve its ability to resist and suppress inflammation [31]. Furthermore, AKK bacteria can ameliorate colitis in TLR4-deficient mice by increasing the proportion of ROR γ t + Treg cells and activating their immune response [32]. AKK bacteria can also induce the secretion of specific cytokines by human immune cells through the a15:0-i15:0 PE (A diacyl phosphatidylethanolamine with two branched chains) molecule and can reset the activation threshold of dendritic cells, which regulates subsequent immune stimulation (such as LPS) to trigger specific immune responses in human immune cells and enhance intestinal immune function [33]. *Proteobacteria* are usually closely related to intestinal health and immune function, and their significant differences may have a negative impact on the host immune response and metabolism [29]. In patients with severe AP, the homeostasis of the intestinal flora is unbalanced (a decrease in probiotics and an increase in opportunistic

pathogens), which causes damage to the intestinal mucosal barrier (a decrease in SCFA secretion and destruction of the intestinal epithelium). An imbalance in inflammation-related flora exacerbates intestinal inflammation, and disorders of the intestinal flora also affect intestinal immune function. Ultimately influenced by various factors, AP patients tend to develop a more severe disease state.

Differentially abundant metabolites and metabolic pathways cause damage to the intestinal mucosal barrier and disrupt energy metabolism that leads to severe AP

Patients with AP presented significant changes in different metabolites, including choline, myo-inositol, nicotinic acid, L-carnitine, trans-cinnamate, 5-aminopentanoic acid, naringenin, and cholic acid, at various disease stages (A vs. R). These differentially abundant metabolites may reflect variations in pathophysiological, metabolic, and inflammatory processes between active and remission patients [34], which provides valuable insights into the biological differences among different disease stages of AP. The significant decrease in choline may reflect the destruction of cell membrane integrity in AP patients during the disease phase and may also locally affect the intestinal barrier or mucosal immune balance [35, 36]. Changes in myo-inositol may indicate alterations in cell signalling pathways in patients at different stages of the disease [37], whereas decreased nicotinic acid may be associated with metabolic abnormalities and cell damage [38]. Moreover, a decrease in nicotinic acid may be related to metabolic abnormalities and cell damage [39]. In addition, L-carnitine plays a key role in fatty acid metabolism [40], and significant changes in L-carnitine may reflect the different requirements of lipid metabolism in active and remission patients, whereas the differences in trans-cinnamate may be related to the oxidative stress levels [41]. These findings suggest that the antioxidant response is altered in patients in the active and recovery stages, and it has certain antibacterial activity and anti-inflammatory effects [42]. Among pathways that differed between the two groups, the most significant pathway was primary bile acid biosynthesis, which plays a pivotal role in synthesizing bile acids and is an integral component of lipid metabolism. In the ascorbate and aldarate metabolism pathway, D-glucuronic acid can undergo a series of enzymatic conversions to generate ascorbic acid and thereby exert inhibitory effects on inflammatory responses [43]. This analysis revealed that during the active period of the disease, differentially abundant metabolites/pathways may lead to intestinal mucosal barrier damage, cell damage, abnormal energy metabolism, and a weakened anti-inflammatory ability in AP patients. These changes are closely related to the

clinical manifestations and outcomes of AP patients and may constitute a pathway for progression to severe pancreatitis. If patients do not receive a timely treatment or ideal intervention, severe pancreatitis is highly likely to develop.

Multiple differentially abundant metabolites, including isoproterenol, muricholic acid, and cis-aconitic acid, were identified in patients with different severities (M vs. S) of AP. Previous studies have shown that bile acids and their metabolites are associated with the cytopathological process of pancreatitis [44, 45]. Muricholic acid is a specific type of bile acid. Studies have shown that bile acids act as signalling molecules by targeting receptors and regulating a variety of pathophysiological downstream processes such as metabolism, inflammation and immunity [46–48]. Prof. Ning Sun's team reported that the activation of farnesoid X receptor (FXR) in pancreatic acinar cells could restore impaired autophagy in pancreatitis by promoting the target gene OSGIN1 and the clearance of autophagosomes and thereby protect against pancreatitis [49]. Studies have shown that FXR can repair damage to the intestinal vascular mucosal barrier by activating the Wnt/ β -catenin signalling pathway in endothelial cells [48]. Furthermore, bile acids have been detected in plasma extracellular vesicles in severe acute pancreatitis [50], which suggests that they may play a role in the development of pancreatitis or can be used as a predictor of AP severity. In the severe group, muricholic acid, which is a specific type of bile acid, can promote the clearance of autophagosomes by binding to FXR and protecting against pancreatitis [49]. In addition, studies have shown that muricholic acid can also be detected in the plasma of SAP patients and may be an important metabolite for predicting the severity of AP [51], which provides a new and reliable therapeutic target and a targeted metabolite for the early prediction of pancreatitis.

Metabolic pathways associated with different disease severities include the TCA cycle (tricarboxylic acid cycle) and glyoxylate and dicarboxylate metabolism. The TCA cycle is the main pathway by which the body obtains energy, and it also provides raw materials for the synthesis of some substances in the body (such as succinyl coenzyme A for haem) [52]. Glyoxylate and dicarboxylate metabolism is usually involved in the biosynthesis of carbohydrates [53]. Changes in these metabolites may reveal differences in energy production and metabolic balance between mild and severe patients. In particular, the TCA cycle is one of the key pathways for intracellular energy production, and glyoxylate and dicarboxylate metabolism is involved in maintaining metabolic balance in organisms. These

metabolic changes suggest that pancreatitis leads to increased energy demand or relatively insufficient energy supply, which often results in a hyperdynamic and hypermetabolic stress state [54]. This change may be due to the lack of acetyl-CoA in mitochondria and is caused by insufficient oxidative phosphorylation and fatty acid oxidation in the body in pancreatitis [55], which results in ATP generation disorders [56]. These disorders reduce the energy provided to cells and cause damage to or necrosis of pancreatic acinar cells and lead to the progression of AP in patients. However, a reduction in the energy supply of intestinal cells may lead to further damage to the cell membrane and cause changes, such as intestinal mucosal barrier damage and dysbiosis, which may lead to severe pancreatitis.

Overall, we explored differences in the gut microbiota and metabolites of AP patients cross-sectionally and longitudinally and provided further clarification of the potential mechanisms of AP severity, which offers new insights for a comprehensive understanding of the pathogenesis, prevention, and personalized treatment of AP such as faecal microbiota transplantation (FMT). We plan to conduct further studies on these issues including verification of the clinical data in additional cases and animal experiments or culture omics methods.

Author contribution

XX, XH and DW participated in the study conception and design. ZW, MG and SY have performed analysis and interpretation of the data. YC, JC, ZH, TW and XL were involved in data analysis and interpretation. ZW, MG and JC prepared the manuscript and figures. MG conducted the statistical analysis. ZW, DW and XX edited, critically read, and revised the manuscript. All authors contributed to the article and approved the submitted version.

Funding

This work was supported by the cultivation project of Zhuhai People's Hospital (2019PY-30) and the Medical and Health Project of Zhuhai Science and Technology Plan (20191208E030029).

Data availability

No datasets were generated or analysed during the current study.

Declarations

Competing interests

The authors declare no competing interests.

Received: 2 February 2024 Accepted: 2 October 2024

Published online: 30 October 2024

References

- CPS Association. Chinese society of surgery, Chinese medical association. *Zhonghua Wai Ke Za Zhi*. 2021;59(7):578–87.
- Mederos MA, Reber HA, Girgis MD. Acute pancreatitis: a review. *JAMA*. 2021;325(4):382–90.
- Hammad AY, Ditillo M, Castanon L. Pancreatitis. *Surg Clin North Am*. 2018;98(5):895–913.
- Villaseñor A, Kinross JM, Li JV, et al. 1H NMR global metabolic phenotyping of acute pancreatitis in the emergency unit. *J Proteome Res*. 2014;13(12):5362–75.
- Ma C, Tian B, Wang J, et al. Metabolic characteristics of acute necrotizing pancreatitis and chronic pancreatitis. *Mol Med Rep*. 2012;6(1):57–62.
- Xiao H, Huang JH, Zhang XW, et al. Identification of potential diagnostic biomarkers of acute pancreatitis by serum metabolomic profiles. *Pancreatology*. 2017;17(4):543–9.
- Zhang L, Shi J, Du D, et al. Ketogenesis acts as an endogenous protective programme to restrain inflammatory macrophage activation during acute pancreatitis. *EBioMedicine*. 2022;78:103959.
- Li H, Xie J, Guo X, et al. Bifidobacterium spp. and their metabolite lactate protect against acute pancreatitis via inhibition of pancreatic and systemic inflammatory responses. *Gut Microbes*. 2022;14(1):2127456.
- Mosca A, Leclerc M, Hugot JP. Gut microbiota diversity and human diseases: should we reintroduce key predators in our ecosystem? *Front Microbiol*. 2016;7:455.
- Lu WW, Chen X, Ni JL, et al. The role of gut microbiota in the pathogenesis and treatment of acute pancreatitis: a narrative review. *Ann Palliat Med*. 2021;10(3):3445–51.
- Zhu Y, Mei Q, Fu Y, et al. Alteration of gut microbiota in acute pancreatitis and associated therapeutic strategies. *Biomed Pharmacother*. 2021;141:111850.
- Zhu Y, He C, Li X, et al. Gut microbiota dysbiosis worsens the severity of acute pancreatitis in patients and mice. *J Gastroenterol*. 2019;54(4):347–58.
- Ashraf R, Shah NP. Immune system stimulation by probiotic microorganisms. *Crit Rev Food Sci Nutr*. 2014;54(7):938–56.
- Banks PA, Bollen TL, Dervenis C, et al. Classification of acute pancreatitis–2012: revision of the Atlanta classification and definitions by international consensus. *Gut*. 2013;62(1):102–11.
- Pancreatic Diseases Group of Chinese Society of Gastroenterology, Editorial Board of Chinese Journal of Pancreatic Diseases, Editorial Board of Chinese Journal of Digestion. Chinese guidelines for the diagnosis and treatment of acute pancreatitis (2019, Shenyang). *J Clin Hepatol Biliary Dis*. 2019, 35(12):2706–2711.
- Magoč T, Salzberg SL. FLASH: fast length adjustment of short reads to improve genome assemblies. *Bioinformatics*. 2011;27(21):2957–63.
- Callahan BJ, McMurdie PJ, Rosen MJ, Han AW, Johnson AJ, Holmes SP. DADA2: high-resolution sample inference from Illumina amplicon data. *Nat Methods*. 2016;13(7):581–3.
- Bolyen E, Rideout JR, Dillon MR, et al. Reproducible, interactive, scalable and extensible microbiome data science using QIIME 2. *Nat Biotechnol*. 2019;37:852–7.
- Seegmiller J, Moshin J, Taylor AM et al. A highly selective, robust and simple accurate mass MS/MS drug screening method using the TripleTOF 5600(+) System[C]//13th International Congress of Therapeutic Drug Monitoring and Clinical. 2013.
- Want EJ, Masson P, Michopoulos F, et al. Global metabolic profiling of animal and human tissues via UPLC-MS. *Nat Protoc*. 2012;8(1):17–32.
- Smith CA, Want EJ, O'Maille G, Abagyan R, Siuzdak G. XCMS: processing mass spectrometry data for metabolite profiling using nonlinear peak alignment, matching, and identification. *Anal Chem*. 2006;78(3):779–87.
- Kuhl C, Tautenhahn R, Böttcher C, Larson TR, Neumann S. CAMERA: an integrated strategy for compound spectra extraction and annotation of liquid chromatography/mass spectrometry data sets. *Anal Chem*. 2012;84(1):283–9.
- Wen B, Mei Z, Zeng C, Liu S. metaX: a flexible and comprehensive software for processing metabolomics data. *BMC Bioinform*. 2017;18(1):183.
- Van den Berg FF, Hugenholtz F, Boermeester MA, Zaborina O, Alverdy JC. Spatioregional assessment of the gut microbiota in experimental necrotizing pancreatitis. *BJS Open*. 2021;5(5):zrab061.
- Su X, Gao Y, Yang R. Gut microbiota-derived tryptophan metabolites maintain gut and systemic homeostasis. *Cells*. 2022;11(15):2296.

26. Kamada N, Kim YG, Sham HP, et al. Regulated virulence controls the ability of a pathogen to compete with the gut microbiota. *Science*. 2012;336(6086):1325–9.
27. Hu H, Yao Y, Liu F, et al. Integrated microbiome and metabolomics revealed the protective effect of baicalin on alveolar bone inflammatory resorption in aging. *Phytomedicine*. 2024;124:155233.
28. Huang YH, Wang ZJ, Ma HJ, Ji SL, Chen ZP, Cui ZK, Chen JS, Tang SB. Dysbiosis and implication of the gut microbiota in diabetic retinopathy. *Front Cell Infect Microbiol*. 2021;11:646348.
29. Patel BK, Patel KH, Bhatia M, et al. Gut microbiome in acute pancreatitis: a review based on current literature. *World J Gastroenterol*. 2021;27(30):5019.
30. Burger-van Paassen N, Vincent A, Puiman PJ, et al. The regulation of intestinal mucin MUC2 expression by short-chain fatty acids: implications for epithelial protection. *Biochem J*. 2009;420(2):211–9.
31. Cani PD, Depommier C, Derrien M, et al. Akkermansia muciniphila: paradigm for next-generation beneficial microorganisms. *Nat Rev Gastroenterol Hepatol*. 2022;19:625–37.
32. Liu Y, Yang M, Tang L, et al. TLR4 regulates ROR γ t+regulatory T-cell responses and susceptibility to colon inflammation through interaction with Akkermansia muciniphila. *Microbiome*. 2022;10(1):98.
33. Bae M, Cassilly CD, Liu X, et al. Akkermansia muciniphila phospholipid induces homeostatic immune responses. *Nature*. 2022;608(7921):168–73.
34. Feng YC, Wang M, Zhu F, et al. Study on acute recent stage pancreatitis. *World J Gastroenterol: WJG*. 2014;20(43):16138.
35. Ying M, Qifei W, Zhimin LYU. Cholesterol metabolism and tumor. *J Zhejiang Univ (Med Sci)*. 2021;50(1):23.
36. Liu LW, Xie Y, Li GQ, et al. Gut microbiota-derived nicotinamide mononucleotide alleviates acute pancreatitis by activating pancreatic SIRT3 signalling. *Br J Pharmacol*. 2023;180(5):647–66.
37. Chhetri DR. Myo-inositol and its derivatives: their emerging role in the treatment of human diseases. *Front Pharmacol*. 2019;10:1172.
38. Mousa TY, Mousa O Y. Nicotinic Acid Deficiency. 2020.
39. Wu MZ, Cai HY. Effect and requirement of niacin. *Chin Feed*. 2001;14:16–8.
40. Chamberlain S. ACNP 60th annual meeting: panels, mini-panels and study groups. *Neuropsychopharmacology*. 2021;46(Suppl 1):1–71.
41. Murakami Y, Kawata A, Suzuki S, Fujisawa S. Cytotoxicity and pro-/anti-inflammatory properties of cinnamates, acrylates and methacrylates against RAW264.7 cells. *In Vivo*. 2018;32(6):1309–22.
42. Zhang CL, Song KK, Chen XR, et al. Antibacterial activity of cinnamic acid and its derivatives. *J Xiamen Univ Nat Sci Edit*. 2006;45(B05):4.
43. Wang J, Bai X, Peng C, et al. Fermented milk containing *Lactobacillus casei* Zhang and *Bifidobacterium animalis* ssp. *lactis* V9 alleviated constipation symptoms through regulation of intestinal microbiota, inflammation, and metabolic pathways. *J Dairy Sci*. 2020;103(12):11025–38.
44. Ye S, Si C, Deng J, et al. Understanding the effects of metabolites on the gut microbiome and severe acute pancreatitis. *Biomed Res Int*. 2021;2021:1516855.
45. Tran QT, Sandler M, Doller J, et al. Role of bile acids and bile salts in acute pancreatitis: from the experimental to clinical studies. *Pancreas*. 2021;50(1):3.
46. Varma VR, Wang Y, An Y, et al. Bile acid synthesis, modulation, and dementia: a metabolomic, transcriptomic, and pharmacoepidemiologic study. *PLoS Med*. 2021;18(5): e1003615.
47. Guan B, Tong J, Hao H, et al. Bile acid coordinates microbiota homeostasis and systemic immunometabolism in cardiometabolic diseases. *Acta Pharm Sin B*. 2022;12(5):2129–49.
48. Guo D, He L, Gao Y, et al. Obeticholic acid derivative, T-2054 suppresses osteoarthritis via inhibiting NF- κ B-signaling pathway. *Int J Mol Sci*. 2021;22(8):3807.
49. Zheng Y, Sun W, Wang Z, et al. Activation of pancreatic acinar FXR protects against pancreatitis via osgin1-mediated restoration of efficient autophagy. *Research (Wash D C)*. 2022;2022:9784081.
50. Mouries J, Brescia P, Silvestri A, et al. Microbiota-driven gut vascular barrier disruption is a prerequisite for non-alcoholic steatohepatitis development. *J Hepatol*. 2019;71(6):1216–28.
51. Zhu Q, Yuan C, Dong X, et al. Bile acid metabolomics identifies chenodeoxycholic acid as a therapeutic agent for pancreatic necrosis. *Cell Rep Med*. 2023;4(12):101304.
52. Krebs HA, Salvin E, Johnson WA, et al. The formation of citric and α -ketoglutaric acids in the mammalian body. *Biochem J*. 1938;32(1):113–7.
53. Zeb A, Liu W, Meng L, et al. Effects of polyester microfibers (PMFs) and cadmium on lettuce (*Lactuca sativa*) and the rhizospheric microbial communities: a study involving physio-biochemical properties and metabolomic profiles. *J Hazard Mater*. 2022;424(Pt C):127405.
54. Ioannidis O, Lavrentieva A, Botsios D. Nutrition support in acute pancreatitis. *JOP*. 2008;9(4):375–90.
55. Zelber-Sagi S, Toker S, Armon G, et al. Elevated alanine aminotransferase independently predicts new onset of depression in employees undergoing health screening examinations. *Psychol Med*. 2013;43(12):2603–13.
56. Mukherjee R, Mareninova OA, Odnokova IV, et al. Mechanism of mitochondrial permeability transition pore induction and damage in the pancreas: inhibition prevents acute pancreatitis by protecting production of ATP. *Gut*. 2016;65(8):1333–46.

Publisher's Note

Springer Nature remains neutral with regard to jurisdictional claims in published maps and institutional affiliations.